THE JOURNAL OF BIOLOGICAL CHEMISTRY VOL. 282, NO. 25, pp. 18162–18172, June 22, 2007

Identification of a Novel Prostaglandin Reductase Reveals the Involvement of Prostaglandin E_2 Catabolism in Regulation of Peroxisome Proliferator-activated Receptor γ Activation*

Received for publication, March 16, 2007, and in revised form, April 19, 2007 Published, JBC Papers in Press, April 21, 2007, DOI 10.1074/jbc.M702289200

Wen-Ling Chou[‡], Lee-Ming Chuang[§], Chi-Chi Chou[¶‖], Andrew H.-J. Wang[¶‖], John A. Lawson[**], Garret A. FitzGerald[**], and Zee-Fen Chang[‡1]

*From the [‡]Institute of Biochemistry and Molecular Biology, College of Medicine, National Taiwan University, Taipei 100, Taiwan, the [§]Department of Internal Medicine, National Taiwan University Hospital, Taipei 100, Taiwan, the [¶]Institute of Biological Chemistry, Academia Sinica, Taipei 115, Taiwan, the [‖]National Core Facilities for Proteomics Research, Taipei 115, Taiwan, and the **Institute for Translational Medicine and Therapeutics, University of Pennsylvania School of Medicine, Philadelphia, Pennsylvania 19104*

This report identifies a novel gene encoding 15-oxoprostaglandin-Δ^{13}-reductase (PGR-2), which catalyzes the reaction converting 15-keto-PGE_2 to 13,14-dihydro-15-keto-PGE_2. The expression of PGR-2 is up-regulated in the late phase of 3T3-L1 adipocyte differentiation and predominantly distributed in adipose tissue. Overexpression of PGR-2 in cells decreases peroxisome proliferator-activated receptor γ (PPARγ)-dependent transcription and prohibits 3T3-L1 adipocyte differentiation without affecting expression of PPARγ. Interestingly, we found that 15-keto-PGE_2 can act as a ligand of PPARγ to increase co-activator recruitment, thus activating PPARγ-mediated transcription and enhancing adipogenesis of 3T3-L1 cells. Overexpression of 15-hydroxyprostaglandin dehydrogenase, which catalyzes the oxidation reaction of PGE_2 to form 15-keto-PGE_2, significantly increased PPARγ-mediated transcription in a PGE_2-dependent manner. Reciprocally, overexpression of wild-type PGR-2, but not the catalytically defective mutant, abolished the effect of 15-keto-PGE_2 on PPARγ activation. These results demonstrate a novel link between catabolism of PGE_2 and regulation of ligand-induced PPARγ activation.

Peroxisome proliferator-activated receptor γ (PPARγ)[2] plays important roles in adipogenesis, lipid and glucose homeostasis, and macrophage function (1–4). PPARγ is a transcription factor in the nuclear receptor family, binding to the promoter of target genes by forming heterodimer with retinoid X receptor (5). Upon ligand binding, PPARγ releases bound co-repressors and recruits co-activator for transcriptional activation (6, 7). High-affinity synthetic agonists of PPARγ, thiazolidinediones, have been widely used as antidiabetic drugs because of their effects in the regulation of lipid metabolism and their anti-inflammatory effects in adipose tissue (8, 9). Several naturally occurring ligands, many associated with the promotion or resolution of inflammation (10–13), including 15-deoxy-$\Delta^{12,14}$prostaglandin J_2 (15d-PGJ_2) (14, 15), components of oxidized low density lipoprotein such as 9-hydroxyoctadecadienoic acid (HODE), 13-HODE, and 15-hydroxyeicosatetraenoic acid (10, 16), lysophosphatidic acid (17), and nitrolinoleic acid (11), have the capacity to activate PPARγ. The production of prostaglandin E_2 (PGE_2) is elevated in many syndromes of inflammation (13, 18). However, little is known about whether the catabolism of PGE_2 is associated with modulation of PPARγ activity (19).

PGE_2, a short-lived mediator, is inactivated via an oxidation reaction catalyzed by NAD^+-dependent 15-hydroxyprostaglandin dehydrogenase (PGDH), which generates 15-keto-PGE_2, which is, in turn, further catabolized by a reaction catalyzed by NADPH/NADH-dependent 15-oxoprostaglandin-Δ^{13}-reductase (PGR) (20). It has been shown that adipose tissue possesses high activity of both PGDH and PGR, indicating that PGE_2 catabolism is highly active in adipocytes (21). 3T3-L1 preadipocyte cell line has been used as a model for characterizing the events responsible for adipocyte differentiation (22), and PGE_2 is the most abundant prostaglandin produced in 3T3-L1 fibroblasts through the release of arachidonic acid from endogenous phospholipids stores or upon addition of exogenous arachidonic acid (23). Although the levels of PGE_2 decreased upon stimulation of 3T3-L1 adipocyte differentiation, PGE_2 is a major prostaglandin produced in adipocytes (23, 24).

In this report, we used a differential display to identify a novel gene encoding prostaglandin reductase, designated as PGR-2. It is highly expressed in the late phase of 3T3-L1 adipocyte differentiation and is also abundant in adipose tissues. PGR-2 is capable of catabolizing 15-keto-PGE_2, and its overexpression represses the transcriptional activity of PPARγ. Following these

* This work was supported by Grants NSC 95-2732-B-002-006-PAE, NSC 95-2732-B-002-008-PAE, and NSC 95-3112-B-001-014 from the National Science Council of Taiwan (Republic of China) and Grant HL62250 from the United States National Institutes of Health. The costs of publication of this article were defrayed in part by the payment of page charges. This article must therefore be hereby marked "*advertisement*" in accordance with 18 U.S.C. Section 1734 solely to indicate this fact.

[1] To whom correspondence should be addressed: Inst. of Biochemistry and Molecular Biology, College of Medicine, National Taiwan University, No. 1, Sec. 1, Jen-Ai Rd., Taipei 100, Taiwan. Tel.: 886-2-23123456, ext. 8229; Fax: 886-2-23958904; E-mail: ZFCHANG@ha.mc.ntu.edu.tw.

[2] The abbreviations used are: PPARγ, peroxisome proliferator-activated receptor γ; PPRE, PPAR response element; 15d-PGJ_2, 15-deoxy-$\Delta^{12,14}$prostaglandin J_2; HODE, hydroxyoctadecadienoic acid; PGR, 15-oxoprostaglandin-Δ^{13}-reductase; PG, prostaglandin; PGDH, 15-hydroxyprostaglandin dehydrogenase; TG, triglyceride; LBD, ligand-binding domain; GST, glutathione *S*-transferase; FBS, fetal bovine serum; DMEM, Dulbecco's modified Eagle's medium; HPLC, high pressure liquid chromatography; MS, mass spectrometry; MS/MS, tandem MS; ESI, electrospray ionization; DI, dexamethasone and insulin medium; MIX, methylisobutylxanthine; LTB4DH, leukotriene B_4-12-hydroxydehydrogenase.

observations, we further established that 15-keto-PGE_2, an intermediate metabolite within the PGE_2 catabolic pathway, can function as a PPARγ ligand, stimulating mouse fibroblasts differentiation into adipocytes. Correspondingly, overexpression of PGDH also increased PGE_2-dependent activation of PPARγ. Our findings provide new insights into the potential importance of PGE_2 catabolism in the regulation of PPARγ activity.

EXPERIMENTAL PROCEDURES

Materials—Chemicals were purchased from Sigma unless otherwise indicated. All prostaglandins were purchased from Cayman Chemical. BRL49653 was a donation from Glaxo-SmithKline Pharmaceuticals. [^{3}H]BRL49653 was from American Radiolabeled Chemicals. The antibodies were as follows: anti-PPARγ (E-8, Santa Cruz Biotechnology), anti-mouse actin (Chemicon), anti-FLAG (M5; Sigma), and anti-aP2 (Alpha Diagnostic International). Rabbit polyclonal antibodies against the recombinant GST-PGR-2 fusion protein were prepared and purified using GST protein-bound glutathione-Sepharose 4B (Amersham Biosciences). Recombinant human PPARγ-LBD (His-tagged) was purchased from Invitrogen. Expression vectors for GAL4-DBD fusion of PPAR-LBDs (GAL4-PPARs) $UAS_G \times 4$-TK-LUC reporter genes were generously provided by R. M. Evans (Howard Hughes Medical Institute, The Salk Institute for Biological Studies, La Jolla, CA). PPRE × 3-TK-LUC and TK-LUC reporter genes were kindly provided by C. K. Glass (University of California San Diego, La Jolla, CA). pGEX-5X3-SRC1$^{568-781}$ plasmid was kindly provided by B. Desvergne (University of Lausanne, Lausanne, Switzerland).

Cell Culture—3T3-L1 fibroblasts were maintained in Dulbecco's modified Eagle's medium (DMEM; high glucose) plus 10% calf serum. Two days after confluence, differentiation was induced by the addition of DMEM containing 10% fetal bovine serum (FBS), 172 nM insulin, 1 μM dexamethasone, and 0.5 mM methylisobutylxanthine for 2 days. The medium was then replaced with DMEM containing 10% FBS and 0.4 μM insulin for an additional 2 days of incubation followed by switching to DMEM plus 10% FBS for full differentiation in 2–3 days. The degree of differentiation was monitored by using Oil-Red O staining and triglyceride (TG) assay (GPO-Trinder; Sigma). 293T cells were cultured in DMEM in the presence of 10% FBS.

Reverse Transcription-Polymerase Chain Reaction—Total RNA was isolated from 3T3-L1 cells at various times throughout differentiation and was reverse transcribed with Supertranscript II (Invitrogen). Semiquantitative PCR amplification was performed for PGR-2 (sense primer, 5′-TAA GTC AGA TGA ATG AGA ACA G-3′; antisense primer, 5′-AAC CAC TGA CTC AGC TGT AG-3′) and 36B4 (sense primer, 5′-CAT GAT GCG CAA GGC TAT CAG-3′; antisense primer, 5′-GAA GGT GTA CTC AGT CTC CA-3′).

Cloning of Mouse PGR-2 cDNA—Mouse PGR-2 was cloned from cDNA of 3T3-L1 adipocyte using PCR amplification (sense primer, 5′-CGG TAT AGC TTG GGA CGC TA-3′; antisense primer, 5′-TGC ATG TTA AGA ATC TTT GTG G-3′) and ligated into a pGEM-T easy vector (Promega) to generate the pTE-PGR-2 construct. The coding region of PGR-2 was then subcloned to the pCMV-Tag2B expression vector (Stratagene). A PCR reaction was carried out for the construction of pFLAG-PGR-2 using pTE-PGR-2 as a template and two primers (forward primer, 5′-AAC TGA AGC TTC AAG TGA TGA TCA TA-3′, where the start codon is underlined; and reverse primer, 5′-AGC TCT CCC ATA TGG TCG ACC T-3′) to generate a HindIII-SalI DNA fragment of PGR-2. This DNA fragment was cloned into the HindIII-SalI sites of pCMV-Tag2B, yielding pFLAG-PGR-2. The HindIII-XhoI fragment of the pFLAG-PGR-2 was inserted into the SmaI-XhoI sites of pGEX-4T-3 vector (Amersham Biosciences) to yield the pGEX-PGR-2 construct, which was used for the generation of the GST-PGR-2 fusion protein. The HindIII-SalI fragment of the pFLAG-PGR-2 was inserted into the EcoRV-SalI sites of pEGFP-C1 vector (BD Biosciences-Clontech) to create the pEGFP-PGR-2 construct. Site-directed mutagenesis of pGEX-PGR-2, pFLAG-PGR-2, and pEGFP-PGR-2 was performed to generate the PGR-2/Y259F catalytically defective mutant using the QuikChange kit (Stratagene) with the following mutagenic primers (mutated sites are underlined): forward primer, 5′-GGT CAG ATT TCT CAG TTC AGT AAC GAT GTG CCC-3′; reverse primer, 5′-GGG CAC ATC GTT ACT GAA CTG AGA AAT CTG ACC-3′.

Cloning of Mouse PGDH cDNA—NAD^+-dependent PGDH was cloned from the cDNA of mouse kidney using PCR amplification (sense primer, 5′-AGT CGG ATC CAT GCA CGT GAA CG-3′, where the start codon is underlined; antisense primer, 5′-CAG TCT CGA GTT ATG GAG CTT TTA C-3′) to generate a BamHI-XhoI DNA fragment of PGDH. This DNA fragment was cloned into the BamHI-XhoI sites of pCMV-Tag2B to yield the pFLAG-PGDH construct.

Expression and Purification of Recombinant PGR-2—An *Escherichia coli* strain XL1-blue was transformed with the plasmid pGEX-PGR-2 to generate the recombinant protein of PGR-2 for the enzyme assay, and the recombinant protein was induced with 0.1 mM isopropyl-1-thio-β-D-galactoside at 25 °C overnight. GST-PGR-2 recombinant protein was purified with a glutathione-Sepharose column according to the manufacturer's instructions (Amersham Biosciences).

Enzymatic Assay for PGR-2—PGR-2 activity assay was carried out in a mixture containing 0.1 M Tris-HCl (pH 7.4), 0.5 mM NADPH, and the substrate 15-keto-PGE_1, 15-keto-PGE_2, 15-keto-$PGF_{1\alpha}$, or 15-keto-$PGF_{2\alpha}$ in a total volume of 100 μl. The reaction was started by adding 5 μg of purified GST-PGR-2 protein and incubated at 37 °C for 30 min. NADPH remaining after the reaction was oxidized by adding 200 μl of color reagent (790 μM indonitrotetrazolium chloride, 60 μM phenazene methosulfate, and 1% Tween 20) at 37 °C in the dark for 10 min followed by adding 700 μl of phthalate buffer (pH 3.0) to stop the reaction. The colorimetric reaction is based on the fact that indonitrotetrazolium can react with NADPH in the presence of phenazene methosulfate to produce formazans (25). The absorbance of formazans was measured at 490 nm with a spectrophotometer. One unit of the enzyme was defined as the amount of enzyme catalyzing the production of 1 μmol $NADP^+$/min. The apparent K_m and V_{max} values were based on Michaelis-Menten kinetics and calculated by Eadie-Hofstee regression using GraphPad Prism software (version 4.0). All values presented are the means of three or more measurements.

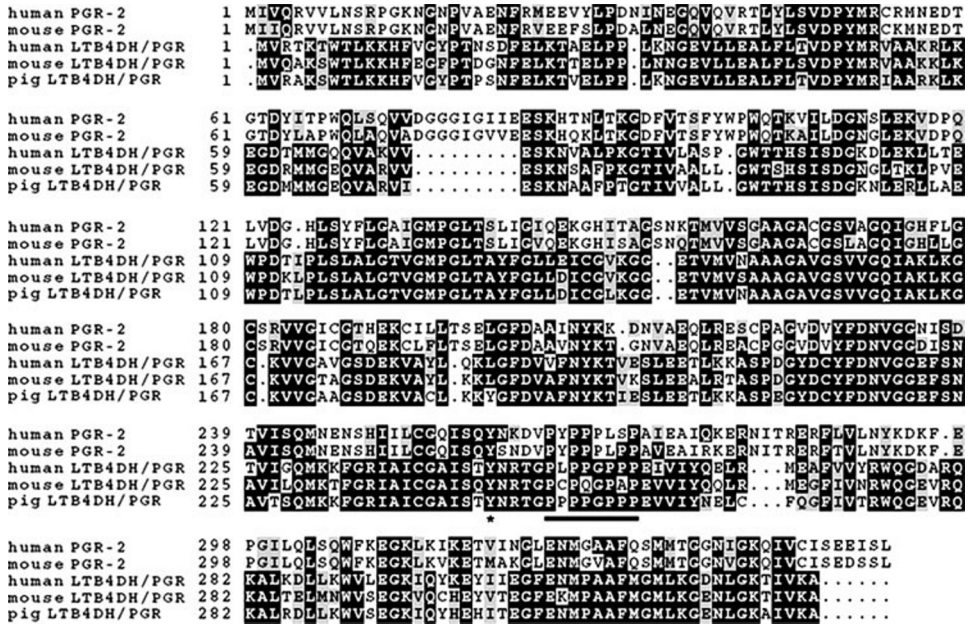

FIGURE 1. **Amino acid sequence alignment of PGR-2 and LTB4DH/PGR.** Human and mouse sequences for PGR-2 and LTB4DH/PGR were aligned with ClustalW and Prettybox. Human and mouse sequences for PGR-2 and LTB4DH/PGR proteins share 86 and 80% identity, respectively. The orthologue of LTB4DH/PGR in pig was cloned separately from kidney and lung (GenBank™ accession numbers NM_214385 and U87622, respectively) (26, 27). The Tyr residue (denoted by an *asterisk*), which is the catalytic site of PGR, is conserved in both PGR-2 and LTB4DH/PGR (28). A proline-rich region with a possible Src homology 3 domain recognition site is indicated by a *bold line*.

Prostaglandin Extraction—Samples after *in vitro* PGR-2 enzyme reaction were acidified to pH 4.0 by 0.5 M citric acid and extracted on C_{18} solid-phase extraction cartridges (Cayman Chemical). After the cartridges were washed with water and hexane, prostaglandins were eluted with ethyl acetate containing 1% methanol. The 293T cells expressing PGDH and PGR-2 were incubated in 10 μM PGE_2 and 10 μM [$^2H_4$]PGE_2 for 18 h to extract intracellular PGE_2 metabolites. Cells were washed twice with phosphate-buffered saline, harvested in homogenization buffer (0.1 M sodium phosphate, pH 7.4, containing 1 mM EDTA and 10 μM indomethacin), and then freeze-thawed in liquid nitrogen. After pH adjustment to pH 4.0 and protein precipitation, the supernatants were loaded onto the C_{18} solid-phase extraction cartridges for prostaglandin elution.

Prostaglandin Analysis—The *in vitro* PGR-2 reaction products were analyzed by nano-ESI-MS and MS/MS. The analytes were directed to the homemade nanosprayer applied with −3.5 kV on the QSTAR-XL hybrid quadrupole time-of-flight mass spectrometer (Applied Biosystems/MDS Sciex). All of the data were acquired and processed using AnalystQS 1.1 with Bioanalyst 1.1 extension. The instrument was calibrated using the fragment ions that resulted from the collision-induced dissociation of Glu-fibrinopeptide B. Full scan mass spectra (MS) were recorded in the negative ion mode in the range of *m*/*z* 100–500. Product ion mass spectra (MS/MS) were obtained for *m*/*z* 351 (13,14-dihydro-15-keto-PGE_2) and *m*/*z* 349 (15-keto-PGE_2) for further identification of the analytes.

Samples were dried under nitrogen, dissolved in 200 μl of 20% acetonitrile, and filtered before analysis for characterization of intracellular PGE_2 metabolites. The instrument used was a Thermo-Finnigan Quantum Ultra AM tandem quadrupole interfaced to a Shimadzu Prominence HPLC system. A 150 mm × 2 mm × 3 μm Luna C_{18} (2) 100A HPLC column (Phenomenex) was maintained at 40 °C. The mobile phase was generated from HPLC-grade water (A) and 5% methanol/95% acetonitrile (B), each containing 0.005% acetic acid adjusted to pH 5.7 with ammonium hydroxide. The flow rate was 200 μl/min using a gradient starting at 20% B and ramping to 60% B in 20 min. Transitions monitored were: [$^2H_4$]-PGE_2, *m*/*z* 355 → 275 at a collision energy (CE) of 18 eV; PGE_2, *m*/*z* 351 → 271, CE 18 eV; [$^2H_4$]-15-keto-PGE_2, *m*/*z* 353 → 165, CE 20 eV; 15-keto-PGE_2, *m*/*z* 349 → 161, CE 20 eV; [$^2H_4$]-13,14-dihydro-15-keto-PGE_2, *m*/*z* 355 → 223, CE 18 eV; 13,14-dihydro-15-keto-PGE_2, *m*/*z* 351 → 219, CE 18 eV. The collision gas was argon, 1.5 millitorr. Source collision-induced dissociation was 12 eV. All compounds were conclusively identified by comparison with synthetic standards (Cayman Chemical).

Transfection and Reporter Assays—One day before transfection, 3T3-L1 fibroblasts were plated at 70–80% confluence, and 293T cells were plated at 30% confluence. After overnight growth at 37 °C, cells were incubated with transfection mixture containing plasmid DNA and Lipofectamine at a 1:6 ratio (Invitrogen). After 24 h of transfection, cells were harvested for determination of luciferase and β-galactosidase activity. Each experiment was repeated three or more times.

Transient Transfection in 3T3-L1 Preadipocytes—Enforced expression of GFP-PGR-2 was performed in post-confluent 3T3-L1 preadipocytes. Cells were transfected with pEGFP-C1, pEGFP-PGR-2, and pEGFP-PGR-2/Y259F construct using Lipofectamine 2000 (Invitrogen) for 5 h according to the manufacturer's instructions. Cells were then washed gently and treated with the standard induction medium for adipocyte differentiation.

Ligand Binding Assays—Ligand binding assays were performed with GST-mPPARγ2 fusion protein, which was expressed in *E. coli* and purified by glutathione-Sepharose affinity chromatography. The protein-bound Sepharose beads were used directly in a binding reaction with 100 nM [^{3}H]BRL49653 in a buffer containing 10 mM Tris-HCl (pH 7.4), 50 mM KCl, and 10 mM dithiothreitol. Competitors or solvent (dimethyl sulfoxide) were added as indicated. Following incubation for 2 h at 4 °C, the PPARγ-Sepharose beads were washed with 10 volumes of ice-cold binding buffer and pulled by centrifugation. The amount of [^{3}H]BRL49653 bound to the beads was measured with a scintillation counter. Each experiment was repeated three or more times.

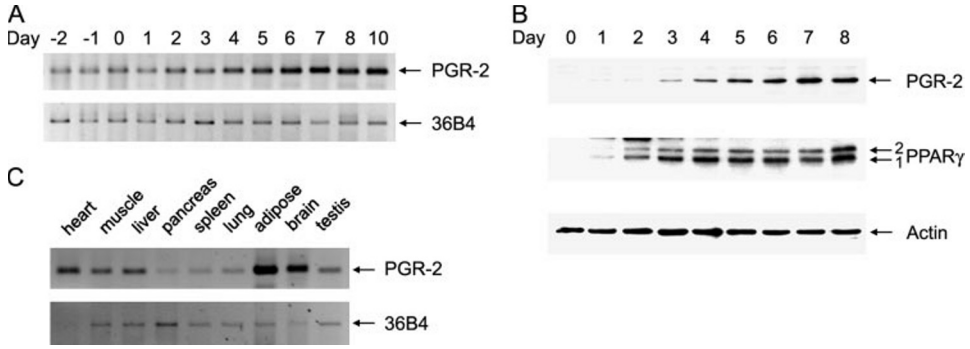

FIGURE 2. **Adipocyte differentiation-dependent PGR-2 gene expression.** *A*, mRNA expression of PGR-2 increases during 3T3-L1 adipocyte differentiation. Post-confluent 3T3-L1 preadipocytes were induced (day 0) to differentiate using the standard differentiation mixture as described. During differentiation, total RNA was isolated from 3T3-L1 cells each day from day 0 to day 10. mRNA expression of PGR-2 was analyzed by reverse transcription-PCR with 36B4 expression as an internal control. *B*, expression of PGR-2 and PPARγ is induced during adipocyte differentiation in different kinetics. Total cellular lysates prepared from post-confluent 3T3-L1 preadipocytes and at various times during differentiation into adipocytes were subjected to Western blot analyses with anti-PGR-2, anti-actin, and anti-PPARγ antibodies. *C*, tissue distribution of mouse PGR-2. Total RNAs from various organs of the mice were extracted. Expression of mRNA of the PGR-2 gene was studied with reverse transcription-PCR using 36B4 expression as an internal control.

Coactivator Recruitment by in Vitro GST Pulldown Assay—GST and GST-SRC1 were expressed in *E. coli*. and purified on the glutathione-Sepharose beads. The purified His-tagged hPPARγ-LBD was preincubated with ligands for 30 min on ice and then mixed with immobilized GST or GST-SRC1 in the pulldown buffer (1× phosphate-buffered saline, 10% glycerol, 0.5% Nonidet P-40). The reactions were incubated overnight at 4 °C after which beads were washed three times in pulldown buffer and boiled in 2× sample buffer. Proteins bound to beads were separated by 11% SDS-PAGE. Blots were then developed with antibodies against PPARγ or GST.

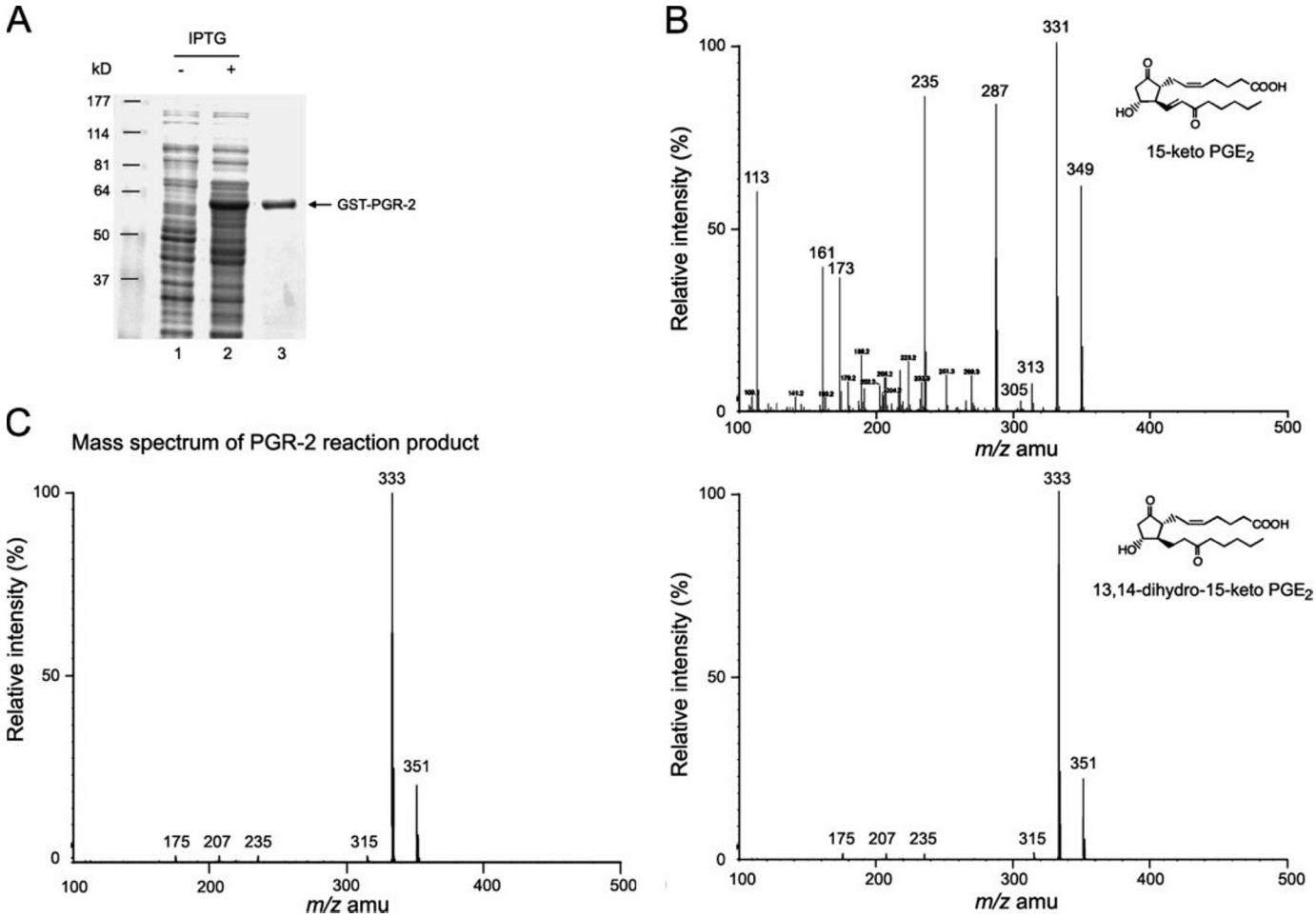

FIGURE 3. **Verification of reaction products using purified PGR-2.** *A*, protein purification of recombinant GST-PGR-2. GST-PGR-2 protein was purified from *E. coli*, and its homogeneity is shown by 10% SDS-PAGE with Coomassie Blue staining. *Lane 1*, total lysate of *E. coli* without isopropyl-1-thio-β-D-galactoside (*IPTG*) induction; *lane 2*, total lysate of *E. coli* with isopropyl 1-thio-β-D-galactopyranoside induction; *lane 3*, purified recombinant protein (2 μg). The molecular size markers are indicated on the *left*. *B*, ESI-MS/MS spectra of standard 15-keto-PGE_2 (*upper panel*) and 13,14-dihydro-15-keto-PGE_2 (*lower panel*) were obtained from fragmentation of the molecular anions of 15-keto-PGE_2 ($[M - H]^- = m/z$ 349) and 13,14-dihydro-15-keto-PGE_2, ($[M - H]^- = m/z$ 351). *C*, ESI-MS/MS spectrum of PGR-2 reaction product. 15-Keto-PGE_2 was incubated with recombinant PGR-2 (5 μg) and 0.5 mM NADPH for 30 min (37 °C) resulting in conversion to 13,14-dihydro-15-keto-PGE_2. The molecular anion of 13,14-dihydro-15-keto-PGE_2 ($[M - H]^- = m/z$ 351) was further fragmented yielding product ions that were 2 proton mass units higher than the corresponding ions in the 15-keto-PGE_2 MS/MS spectrum.

TABLE 1
Specific activities of PGR-2 on various compounds

Substrates	Specific activity[a]
	nmol/min·mg protein
15-Keto-PGE_2	178.4 ± 13.7
15-Keto-PGE_1	115.0 ± 4.8
15-Keto-$PGF_{2\alpha}$	230.9 ± 5.7
15-Keto-$PGF_{1\alpha}$	206.4 ± 6.3
6-Keto-$PGF_{1\alpha}$	ND
$PGF_{2\beta}$	ND
11β-$PGF_{2\alpha}$	ND
13,14-Dihydro-15-keto-PGD_2	ND
13,14-Dihydro-15-keto-PGE_2	ND
13,14-Dihydro-15-keto-$PGF_{2\alpha}$	ND
Leukotriene B_4	ND

[a] ND, non-detectable.

TABLE 2
Enzymatic substrates and kinetic parameters for mouse PGR-2

Substrate	K_m	V_{max}	K_{cat}	K_{cat}/K_m
	μM	*milliunits/mg*[a]	min^{-1}	$mM^{-1}\ min^{-1}$
15-Keto-PGE_2	49.6 ± 5.8	178.4 ± 13.7	11.4 ± 0.9	229.8 ± 17.7
15-Keto-PGE_1	34.4 ± 10.1	115.0 ± 4.8	7.4 ± 0.5	215.1 ± 13.7
15-Keto-$PGF_{2\alpha}$	108.8 ± 13.9	230.9 ± 5.7	14.8 ± 0.4	136.0 ± 3.4
15-Keto-$PGF_{1\alpha}$	59.2 ± 7.4	206.4 ± 6.3	13.2 ± 0.4	222.9 ± 6.8
NADPH	94.6 ± 16	144.7 ± 13.5	9.3 ± 0.9	98.3 ± 9.2

[a] 1 unit = 1 μmol $NADP^+$/min.

Statistical Analyses—Results are expressed as the means ± S.D. Statistical analyses were performed with Student's *t* test for comparison of each effect *versus* control. A p value <0.05 was considered significant.

RESULTS

Identification of PGR-2 by Differential Display during 3T3-L1 Adipocyte Differentiation—The genes differentially expressed in 3T3-L1 cells at day 10 after the induction of adipocyte differentiation were screened using differential display. Among those genes up-regulated, one gene shares 100% identity to NM_029880 as well as AK021033 or AK020666 in the GenBank™. Further blast search of the data base revealed that gene corresponding to NM_029880 encodes a protein sharing a 40% amino acid sequence identity with two paralogous sequences, human NM_012212 and mouse NM_025968, both of which encode the bifunctional leukotriene B_4-12-hydroxydehydrogenase/15-oxoprostaglandin-Δ^{13}-reductase (LTB4DH/PGR or PGR-1) (26–28) (Fig. 1). Based on this similarity, this new gene was designated PGR-2.

Expression of PGR-2 was increased during the differentiation of 3T3-L1 cells at both the mRNA (Fig. 2*A*) and protein levels, with a time lag of ~1 day following the expression of PPARγ (Fig. 2*B*). Among the mouse tissues examined, adipose tissue showed the highest expression of PGR-2 mRNA (Fig. 2*C*). This expression pattern was distinct from that of PGR-1, which is most highly expressed in liver and kidney (26).

Functional Characterization of PGR-2 as a 15-Oxoprostaglandin-Δ^{13}-reductase—To analyze the biochemical function of PGR-2, we cloned and sequenced PGR-2 cDNA from 3T3-L1 adipocytes (see "Experimental Procedures"). We expressed and purified the recombinant mouse PGR-2 as a GST fusion protein from the *E. coli* system to perform an enzymatic assay (Fig. 3*A*). Based on the presence of a conserved domain of putative NADP(H)-dependent oxidoreductase in its amino acid

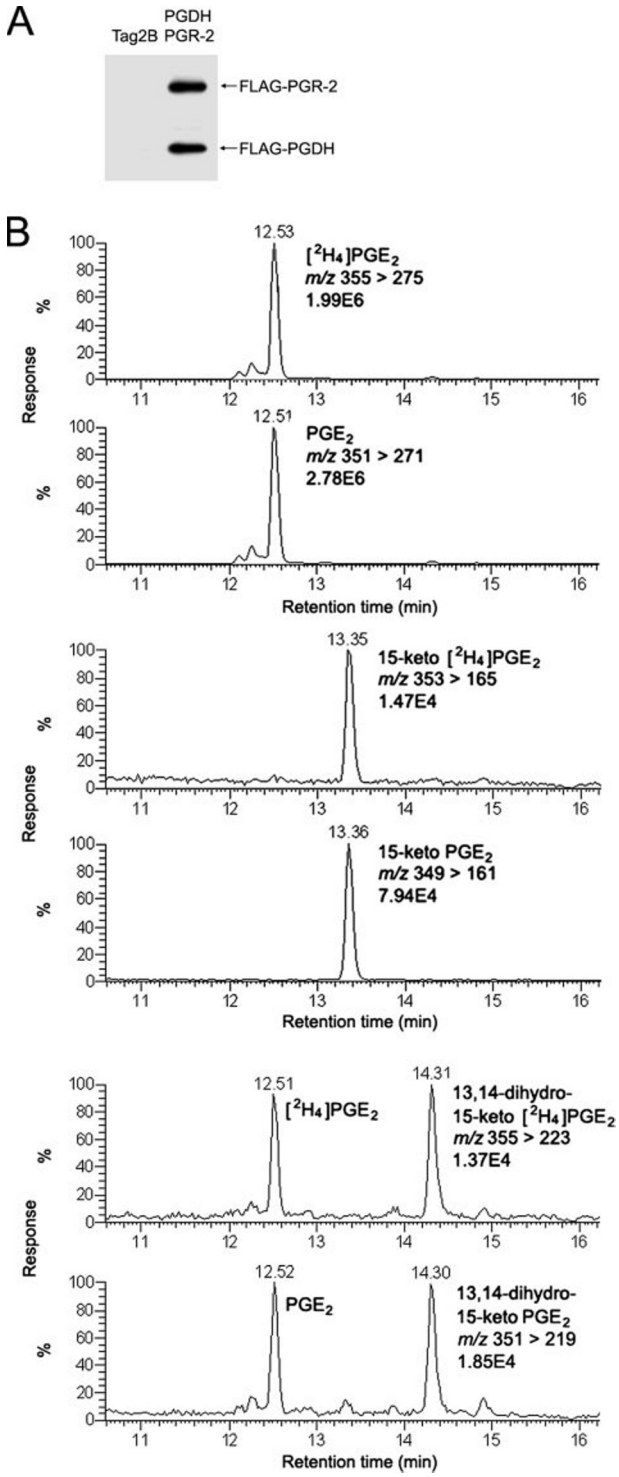

FIGURE 4. **Metabolic conversion of PGE_2 to 13,14-dihydro-15-keto-PGE_2 by coexpressing PGDH and PGR-2 *in vivo*.** *A*, 293T cells were transfected with expression vectors of FLAG-PGDH and FLAG-PGR-2 or with vector alone (*Tag2B*). Expression of FLAG-PGDH and FLAG-PGR-2 in 293T cells was detected by Western blot analyses using anti-FLAG (M5) antibody. *B*, for characterization of PGE_2 metabolites, transfected cells were treated with 10 μM PGE_2 and 10 μM [$^2H_4$]-PGE_2 for 18 h. Intracellular prostaglandins were extracted and analyzed by liquid chromatography-MS/MS. Representative chromatograms of PGE_2, 15-keto-PGE_2, and 13,14-dihydro-15-keto-PGE_2 from 293T cells expressing FLAG-PGDH and FLAG-PGR-2 are shown, respectively. [$^2H_4$]-PGE_2 (*m/z* 355) and PGE_2 (*m/z* 351), retention time 12.5 min; [$^2H_4$]-15-keto-PGE_2 (*m/z* 353) and 15-keto-PGE_2 (*m/z* 349), retention time 13.4 min; [$^2H_4$]-13,14-dihydro-15-keto-PGE_2 (*m/z* 355) and 13,14-dihydro-15-keto-PGE_2 (*m/z* 351), retention time 14.3 min.

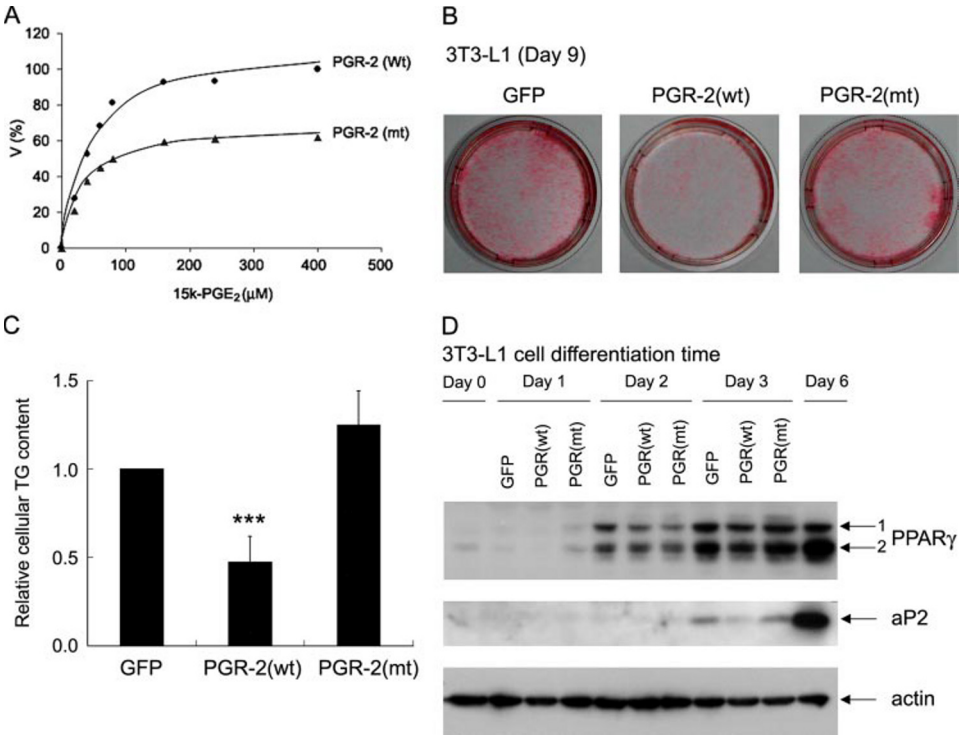

FIGURE 5. **Enforced expression of PGR-2 in the early phase of adipogenesis inhibits the differentiation of 3T3-L1 cells.** *A*, Michaelis-Menten plot of wild-type PGR-2 (*Wt*) and PGR-2/Y259F mutant (*mt*) enzyme reaction with various concentration of 15-keto-PGE_2 (*15k-PGE_2*). Post-confluent 3T3-L1 preadipocytes were transfected with expression vector of GFP, GFP-PGR-2 (*Wt*), and GFP-PGR-2/Y259F (*mt*) as indicated. Following the transfection, cells were induced to differentiate with the standard differentiation mixture as described under "Experimental Procedures." *B*, accumulation of lipid droplets was shown by staining with Oil-Red O at 9 days after induction. *C*, quantitative analyses of total cellular TG content were assayed 9 days after the induction. ***, $p < 0.001$. *D*, after induction, total cellular lysates prepared from day 1 (24 h), day 2 (48 h), and day 3 (72 h) during differentiation were subjected to Western blot analyses with anti-aP2, anti-PPARγ, and anti-actin antibodies. Cell lysates of preadipocyte (*Day 0*) and adipocytes (*Day 6*) were loaded in parallel as controls.

sequence, we measured its prostaglandin reductase activity using different prostaglandins as the substrate. Toward this end, we developed a colorimetric assay by measuring formazan formation from the reduction of the tetrazolium salt in detecting the prostaglandin reductase activity (See "Experimental Procedures").

The results of enzymatic analysis showed that 15-keto-PGE_2, 15-keto-PGE_1, 15-keto-$PGF_{2\alpha}$, and 15-keto-$PGF_{1\alpha}$ were promising substrates, whereas 13,14-dihydro-15-ketoprostaglandins were not. Neither dehydrogenase activity nor LTB4DH activity was associated with PGR-2 (Table 1). Kinetic studies revealed that PGR-2, requiring NADPH but not NADH as a cofactor, had the highest efficiency in converting 15-keto-PGE_2 into 13,14-dihydro-15-keto-PGE_2 (K_{cat}/K_m = 229.8 $mM^{-1}min^{-1}$ compared with 222.9 $mM^{-1}min^{-1}$ for 15-keto-$PGF_{1\alpha}$, 215.1 $mM^{-1}min^{-1}$ for 15-keto-PGE_1, and 136.0 $mM^{-1}min^{-1}$ for 15-keto-$PGF_{2\alpha}$ (as summarized in Table 2)). The reaction product obtained from the incubation of 15-keto-PGE_2 and NADPH with purified PGR-2 was further analyzed by ESI-MS/MS to verify 13,14-dihydro-15-keto-PGE_2 formation in the reaction (Fig. 3*C*). The molecular anion ($[M - H]^- = m/z$ 351) from the reaction product gave the same fragments in the MS/MS spectrum as standard 13,14-dihydro-15-keto-PGE_2, which yielded ions that were 2 proton mass units higher than corresponding ions in the 15-keto-PGE_2 MS/MS spectrum (Fig. 3, *B* and *C*).

We also analyzed the *in vivo* catabolites of PGE_2 through the action of PGDH and PGR-2 in intact cells. To this end, 293T cells were transfected with a control plasmid (Tag2B) or expression vectors of PGDH and PGR-2 and treated with PGE_2 (Fig. 4*A*). Deuterium-labeled PGE_2 was included in the medium for *in vivo* uptake to assure the identity of lipid metabolites for mass spectrometric analysis. Intracellular lipid extracts were prepared from these cells for mass spectrometric analysis. We found that both 15-keto-PGE_2 and 13,14-dihydro-15-keto-PGE_2 could be detected in 293T cells expressing PGDH and PGR-2 (Fig. 4*B*). However, 13,14-dihydro-15-keto-PGE_2 was undetectable in cells transfected with the control vector (data not shown).

The Role of PGR-2 Expression in Adipogenesis—Because the expressed level of PGR-2 was not increased until 3T3-L1 cells had attained late stage differentiation to adipocytes, we then determined whether constitutive expression of PGR-2 would influence adipocyte differentiation. 3T3-L1 cells were transiently transfected with a wild-type expression vector and a catalytically defective GFP-PGR-2, and differentiation was then induced. Based on structural prediction, the conserved Tyr-259 residue in PGR-2 (Fig. 1) might function as the Tyr-245 of PGR-1 that participates in the hydrogen bond network around the 2′-hydroxyl group of the nicotine amide ribose, which interacts with two water molecules in stabilizing an enolate intermediate for the catalysis of 15-keto-PGE_2 reduction (28). The Y259F mutant of PGR-2 was then generated and showed a significant decrease in catalytic efficiency in the reduction reaction of 15-keto-PGE_2 (Fig. 5*A*). We found that ectopic expression of the wild type but not Y259F of GFP-PGR-2 dramatically inhibited adipocyte differentiation, as evaluated by the accumulation of lipid droplets with Oil-Red O staining (Fig. 5*B*), and decreased intracellular TG synthesis by 53% as compared with control cells (Fig. 5*C*). Furthermore, ectopic expression of wild-type GFP-PGR-2, but not the Y259F mutant, significantly reduced the induction of the PPARγ target gene, aP2, whereas the expression level of PPARγ remained unaltered (Fig. 5*D*). These results clearly demonstrate that constitutive expression of functional PGR-2 impairs PPARγ-mediated adipocyte differentiation without affecting the protein expression level of PPARγ.

15-Keto-PGE_2 Is a PPARγ Ligand—The effect of overexpression of PGR-2 on the suppression of adipocyte differentiation (Fig. 5, *B–D*) and the induction pattern of PGR-2 expression (Fig. 2, *A* and *B*) indicates that catabolism of

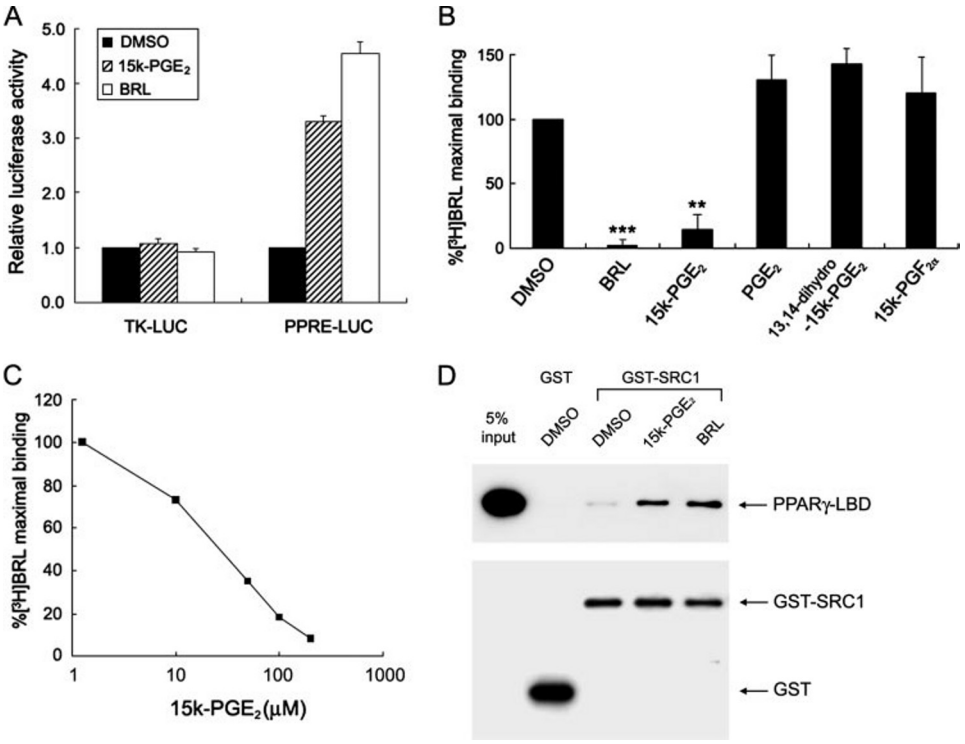

FIGURE 6. **Identification of 15-keto-PGE_2 as a PPARγ ligand.** *A*, 15-keto-PGE_2 (*15k-PGE_2*) increased PPRE-mediated transcription in differentiating 3T3-L1 cells. 3T3-L1 preadipocytes were induced to differentiate with the standard differentiation mixture for 2 days. Cells were then transfected with the PPRE × 3-TK-LUC reporter/TK-LUC reporter and CMV-βGal and treated with dimethyl sulfoxide (*DMSO*), 14 μM 15-keto-PGE_2, or 4.5 μM BRL49653 (*BRL*) in the presence of insulin and FBS for 24 h. The relative luciferase activity was determined after normalization for transfection efficiency with β-galactosidase. *B*, 15-keto-PGE_2 is a PPARγ ligand. *In vitro* ligand binding assays were performed using a GST-mPPARγ2 fusion protein immobilized on glutathione-Sepharose beads and 100 nM [^{3}H]BRL49653 in the presence of vehicle (*DMSO*), 10 μM unlabeled BRL49653, or 100 μM unlabeled PGs (15-keto-PGE_2, PGE_2, 13,14-dihydro-15-keto-PGE_2, and 15-keto-$PGF_{2\alpha}$). **, $p < 0.01$; ***, $p < 0.001$. *C*, dose-response curve for 15-keto-PGE_2 competition of [^{3}H]BRL49653 binding to PPARγ. *D*, 15-keto-PGE_2 enhanced the interaction of PPARγ with SRC1. Bacterially expressed GST-SRC1 was incubated with the purified His-tagged PPARγ-LBD in the presence of dimethyl sulfoxide, 15-keto-PGE_2 (10 μM), or BRL49653 (10 μM). The beads were then washed, and the samples were subjected to SDS-PAGE and immunoblotted for PPARγ and GST.

15-keto-PGE_2 by PGR-2 needs to be suppressed during the early phase of adipocyte differentiation. Because PGE_2 is a major prostaglandin produced in preadipocytes (23, 24) and there is a temporal difference between the expression of PGR-2 and PPARγ during adipogenesis of 3T3-L1 cells (Fig. 2*B*), we raised the question of whether 15-keto-PGE_2, rather than PGE_2, has a functional role in modulating PPARγ activity during adipocyte differentiation. We transiently transfected the PPRE-based reporter gene (PPRE-TK-Luc) into 3T3-L1 that had been induced for differentiation for 2 days (PPARγ expression was induced and the level of PGR-2 was still low) to determine the effect of 15-keto-PGE_2 on PPRE-dependent transcription in the early differentiation stage of 3T3-L1 cells. The addition of 15-keto-PGE_2 to the culture medium of transfected cells was capable of activating transcription of the PPRE-based reporter gene as efficiently as BRL49653, a synthetic ligand of PPARγ (Fig. 6*A*). In parallel experiments, the control reporter gene (TK-Luc) did not respond to 15-keto-PGE_2 or BRL49653. The results suggest that 15-keto-PGE_2 can activate PPRE-dependent transcription.

Next, we tested the ability of 15-keto-PGE_2 to interact with PPARγ *in vitro* using ligand competition assays. 15-Keto-PGE_2, similar to unlabeled BRL49653, was able to compete for the binding of [^{3}H]BRL49653 to PPARγ (Fig. 6*B*), whereas neither PGE_2, 13,14-dihydro-15-keto-PGE_2, nor 15-keto-$PGF_{2\alpha}$ (another substrate of PGR-2) had competitive capacity. Fig. 6*C* further demonstrates the competitive inhibition of [^{3}H]BRL49653 binding to PPARγ by 15-keto-PGE_2 in a dose-dependent manner (the estimated K_d is around 30 μM). We did not test for 15-keto-PGE_1 and 15-keto-$PGF_{1\alpha}$, because the physiological concentrations of PGE_1 and $PGF_{1\alpha}$ are much lower than that of PGE_2 (29).

Because ligand-induced transactivation of PPARγ is achieved by the recruitment of coactivators such as SRC1 and TIF2 (30), we performed an *in vitro* coactivator-dependent receptor ligand assay by incubating the purified recombinant GST-SRC1 with PPARγ-LBD proteins. Similar to BRL49653 as a positive control, inclusion of 15-keto-PGE_2 in the assay enabled PPARγ-LBD to be pulled down by GST-SRC1, indicating that 15-keto-PGE_2 is capable of acting as a ligand in inducing the interaction between SRC1 and PPARγ-LBD (Fig. 6*D*). The same effect of 15-keto-PGE_2 could be seen when the coactivator TIF2 was used for the interaction assay (data not shown). No interaction was detected when GST protein was used for the binding assay. Taken together, these results indicate that 15-keto-PGE_2 is a PPARγ ligand that activates its transcriptional function by promoting co-activator recruitment.

Catabolic Conversion of PGE_2 by Expression of Prostaglandin Dehyrogenase Activates PPARγ—To substantiate the potential role of 15-keto-PGE_2 generation in PPARγ activation, we next tested whether overexpression of PGDH could convert PGE_2 to an activator for PPARγ-mediated transactivation. 293T cells were transfected both with the GAL4 luciferase reporter plasmid (UAS_G) and a vector expressing the ligand-binding domain (LBD) of the mouse PPARγ fused to yeast GAL4 DNA-binding domain with or without the PGDH expression vector (Fig. 7*A*). Overexpression of PGDH had no effect on the transactivation activities of GAL4-PPARγ. Treatment of cells with 10 μM PGE_2 significantly increased GAL4-PPARγ-mediated transcriptional activity in cells expressing PGDH, but not in the cells transfected with the control vector (Fig. 7*B*). Consistent with the catabolic function of PGDH for PGE_2, treatment with 15-keto-PGE_2 also activated GAL4-PPARγ in the cells regardless of PGDH expression (Fig. 7*B*). Furthermore, activation of PPARγ activity in cells expressing PGDH was increased with increasing concentration of PGE_2 (Fig. 7*C*). These results support our

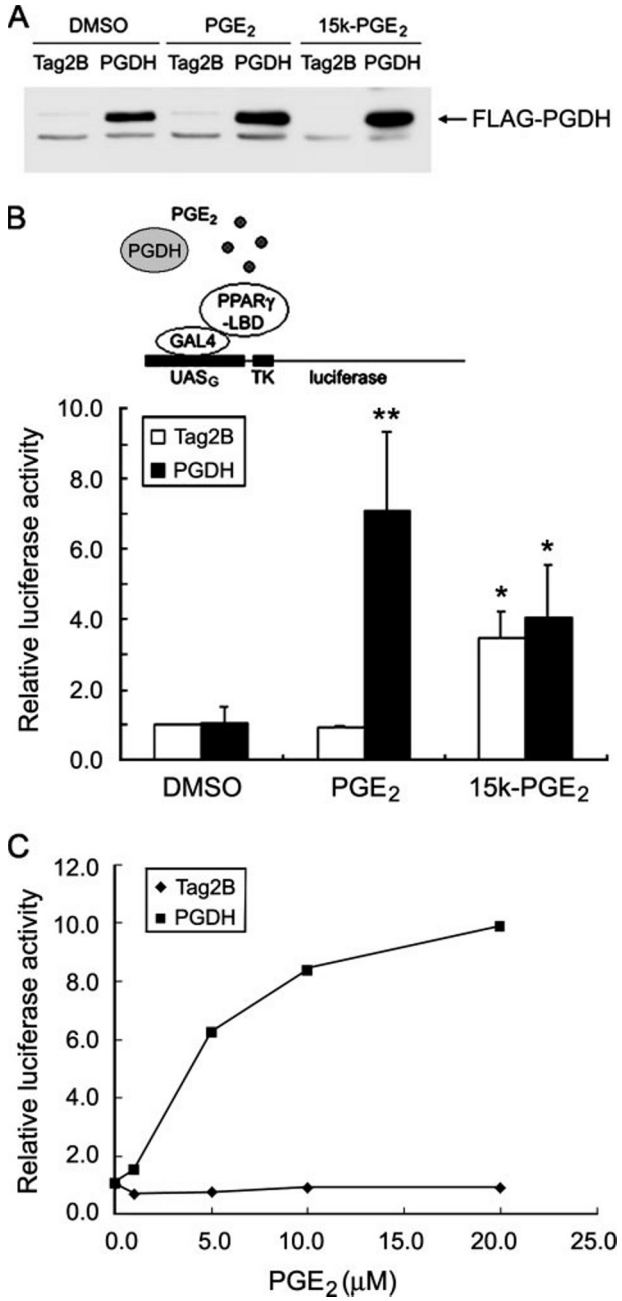

FIGURE 7. **Catabolic conversion of PGE_2 by PGDH overexpression activates PPARγ-mediated transcription.** 293T cells were transfected with UAS_G × 4-TK-LUC (0.7 μg), CMV-βGal (0.1 μg), CMX-GAL4-PPARγ (0.2 μg), and either Tag2B (0.2 μg) or FLAG-PGDH (0.2 μg) as indicated. Following transfection, cells were treated with dimethyl sulfoxide (*DMSO*, vehicle control), 10 μM PGE_2, or 10 μM 15-keto-PGE_2 (*15k-PGE_2*) for 18 h. After treatment, cells were harvested for Western blot analyses (*A*) and luciferase assays (*B*). For Western blot, equal amounts of cell extracts were analyzed to detect the expression of FLAG-PGDH in 293T cells. *, $p < 0.05$; **, $p < 0.01$. *C*, dose-response curve for activation of PPARγ by the expression of PGDH in the presence of PGE_2.

notion that metabolic conversion of PGE_2 to 15-keto-PGE_2 is able to activate PPARγ.

15-Keto-PGE_2 Activates PPARγ-mediated Transcription and Enhances Adipogenesis in 3T3-L1 Cells—The GAL4 luciferase reporter plasmid UAS_G was transfected to 3T3-L1 fibroblasts with GAL4-PPARα, -PPARγ, or -PPARδ to determine the effect of 15-keto-PGE_2 on the transcriptional function of different subtypes of PPAR *in vivo*. Treatment of transfected cells with 15-keto-PGE_2 increased the transactivation activities of GAL4-PPARγ and, to a lesser degree, GAL4-PPARα but not of GAL4-PPARδ (Fig. 8*A*). Moreover, GAL4-PPARγ was more effectively activated by increasing concentrations of 15-keto-PGE_2 than GAL4-PPARα (Fig. 8*B*).

It has been reported that treatment of 3T3-L1 preadipocytes with dexamethasone and insulin (DI) is unable to induce adipocyte differentiation unless methylisobutylxanthine (MIX) is added to DI to stimulate the generation of endogenous PPARγ ligands via the cAMP signaling pathways (31, 32). This system allows us to evaluate the effect of supplementation of PPARγ ligands on the promotion of adipogenesis in the absence of methylisobutylxanthine. As shown in Fig. 8*C*, differentiation did not occur when preadipocytes were incubated in the presence of DI or MIX alone. As expected, the addition of MIX into DI medium gave rise to adipocyte differentiation of 3T3-L1 cells, as manifested by the accumulation of lipid droplets with Oil-Red O staining (Fig. 8*C*) and the quantitative analysis of the intracellular TG content (Fig. 8*D*). Interestingly, the addition of 15-keto-PGE_2 or BRL49653 into DI medium also resulted in adipocyte differentiation to a degree comparable with the effect of MIX in DI medium (Fig. 8, *C* and *D*). We further examined the ability of 15-keto-PGE_2 to induce expression of PPARγ target genes during adipogenesis. Similar to MIX treatment, both 15-keto-PGE_2 and BRL49653 treatment strongly induced the expression of aP2, an adipocyte-specific marker, after 6 days of adipocyte differentiation (Fig. 8*E*). Previous studies have shown that PPARγ ligands are involved in a positive feedback loop to maintain a relatively high expression of PPARγ (31). Consistently, expression of PPARγ was increased in cells cultured in a DI medium supplemented with 15-keto-PGE_2, BRL49653, or MIX. Moreover, the addition of DI with 15-keto-PGE_2 or BRL49653 already induced a prominent aP2 expression in 2 days of treatment, in contrast to a rather weak aP2 induction following the addition of MIX to DI medium (Fig. 8*F*). The differences in aP2 induction in response to 15-keto-PGE_2, BRL49653, and MIX treatment during the early phase of induction of adipogenesis suggest that direct ligand-induced activation of PPARγ by 15-keto-PGE_2 and BRL49653 gave an earlier induction of aP2 than MIX treatment, which requires more time for endogenous ligand generation. Therefore, these data support the proposition that 15-keto-PGE_2 can act as a PPARγ ligand for adipocyte differentiation.

Overexpression of PGR-2 Suppressed 15-Keto-PGE_2-mediated Transactivation of PPARγ—The enzymatic function of PGR-2 in the reduction of 15-keto-PGE_2 led us to determine whether overexpression of PGR-2 could inhibit 15-keto-PGE_2-induced activation of PPARγ. We expressed FLAG-PGR-2 and GAL4-PPARγ in 293T cells at the protein levels comparable with the endogenous levels of PGR-2 and PPARγ in differentiated 3T3-L1 adipocytes (Fig. 9*A*). The addition of 15-keto-PGE_2 to the culture medium without coexpression of FLAG-PGR-2 caused an 8-fold increase in GAL4-PPARγ-mediated transcriptional activation of UAS_G luciferase reporter activity in 293T cells (Fig. 9*B*). Ectopic expression of FLAG-PGR-2

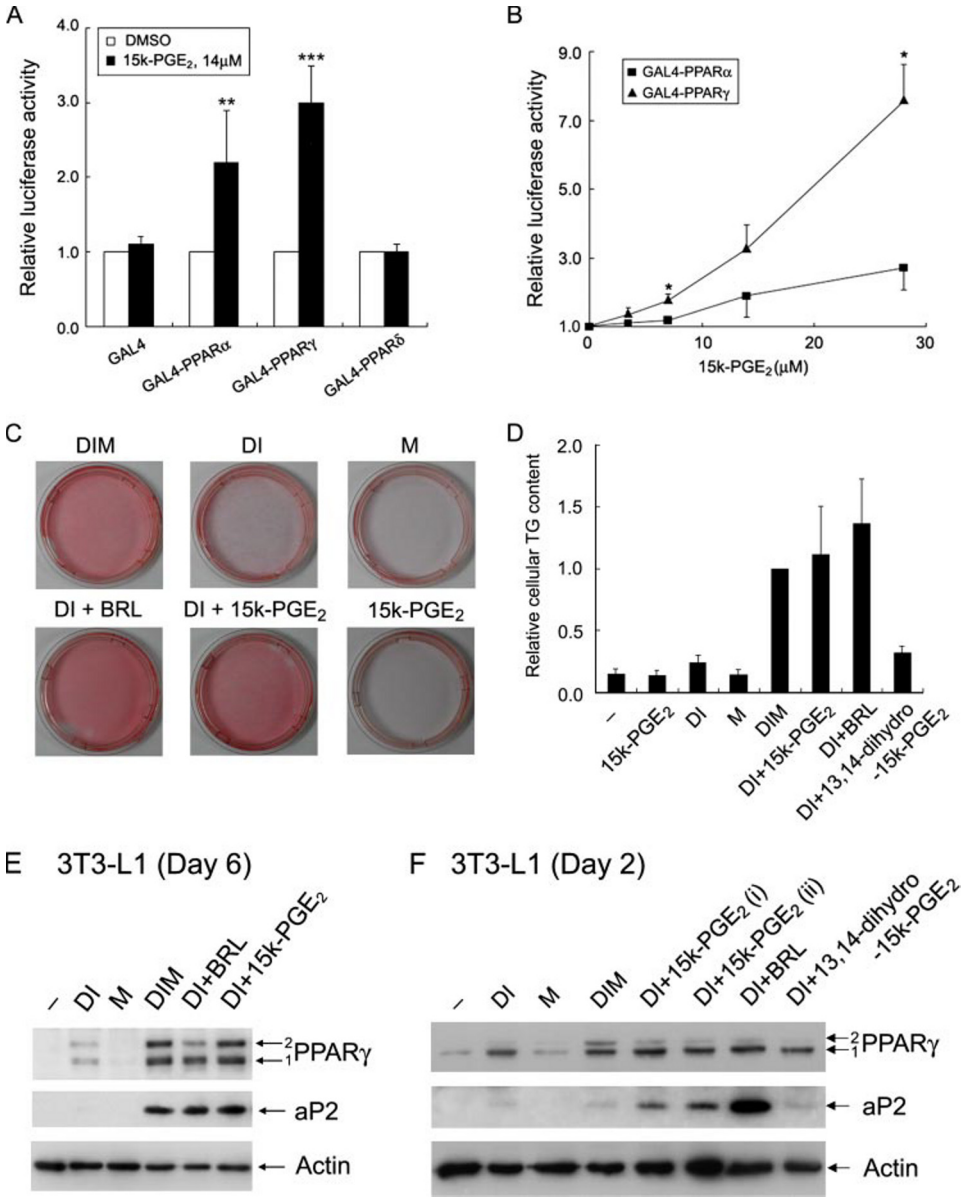

FIGURE 8. **Effect of 15-keto-PGE_2 on PPARγ-mediated transcription and adipogenesis.** *A*, selectivity of 15-keto-PGE_2 (*15k-PGE_2*) on the transactivation of different GAL4-PPARs. 3T3-L1 fibroblasts were transfected with $UAS_G \times 4$-TK-LUC, CMV-β-Gal, and either CMX-GAL4, CMX-GAL4-PPARα, CMX-GAL4-PPARγ, or CMX-GAL4-PPARδ. Following transfection, cells were treated with dimethyl sulfoxide (*DMSO*; vehicle control), or 14 μM 15-keto-PGE_2 for 24 h. The relative luciferase activity was determined after normalization for transfection efficiency with β-galactosidase. **, $p < 0.01$; ***, $p < 0.001$. *B*, dose-response curves of the activation of GAL4-PPARγ and GAL4-PPARα by 15-keto-PGE_2. *, $p < 0.05$. *C* and *D*, 15-keto-PGE_2 enhanced adipocyte differentiation (*C*) and increased cellular TG synthesis (*D*) of 3T3-L1 cells. Post-confluent 3T3-L1 preadipocytes were induced to differentiate with: dexamethasone and insulin (*DI*); methylisobutylxanthine (*M*); 10 μM 15-keto-PGE_2; dexamethasone and insulin in the presence of methylisobutylxanthine (*DIM*), 0.5 μM BRL49653 (*BRL*), 10 μM 15-keto-PGE_2, or 10 μM 13,14-dihydro-15-keto-PGE_2. 15-Keto-PGE_2 and 13,14-dihydro-15-keto-PGE_2 were added every 2 days. At 6 days after induction, the accumulation of lipid droplets was shown by staining with Oil-Red O (*C*) and evaluated by quantitative analyses of the intracellular TG content (*D*). *E*, induction of PPARγ and aP2 genes by 15-keto-PGE_2 in mature 3T3-L1 adipocytes (*Day 6*) was assessed by Western blot analyses. *F*, induction of PPARγ and aP2 genes in the early phase of adipogenesis in 3T3-L1 cells (*Day 2*). Post-confluent 3T3-L1 preadipocytes were induced to differentiation by exposure to the indicated combinations of the adipogenic inducers: DI; methylisobutylxanthine; and dexamethasone and insulin in the presence of 0.5 μM BRL49653, 10 μM 15-keto-PGE_2, or 10 μM 13,14-dihydro-15-keto-PGE_2. For 15-keto-PGE treatment, one set was done with one dose at the induction on day 0 (*i*), and the other with an additional dose administered 24 h after the first dose. 48 h after induction, protein expression of PPARγ, aP2, and actin was detected by Western blot analyses.

markedly suppressed 15-keto-PGE_2-mediated activation of GAL4-PPARγ in the reporter activity in a dose-dependent manner (Fig. 9*B*). Coexpression of Y259F mutant with GAL4-PPARγ no longer decreased the 15-keto-PGE_2-activated transcriptional activity of PPARγ (Fig. 9*B*), indicating that the catalytic activity of PGR-2 is required for negative modulation of 15-keto-PGE_2-dependent transcriptional activation of PPARγ (Fig. 9*C*).

DISCUSSION

The current study presents the first evidence linking the metabolism of 15-keto-PGE_2 to modulation of PPARγ-dependent transcription and adipogenesis. We have shown that catabolic conversion of PGE_2 to 15-keto-PGE_2 by overexpression of PGDH enables PPARγ activation. In addition, we identified PGR-2 as an enzyme that catalyzes the reaction in converting 15-keto-PGE_2 to 13,14-dihydro-15-keto-PGE_2. The amount of PGR-2 expression is abundant in adipose tissue and is up-regulated during 3T3-L1 adipocyte differentiation. Ectopic overexpression of PGR-2 in 3T3-L1 cells dramatically inhibits adipocyte differentiation. These data illuminate the role of PGE_2 catabolism in PPARγ-dependent transcription.

PGE_2 is the major prostaglandin produced by preadipocytes (23), and its catabolism in adipose tissue is highly active (21). Using *in vitro* ligand binding assays, we have proved that 15-keto-PGE_2, a metabolite of PGE_2, is able to compete for binding of a synthetic ligand, BRL49653, to PPARγ. Furthermore, the interaction between SRC1 and PPARγ is induced upon binding of 15-keto-PGE_2 to PPARγ, indicating its ligand function in coactivator recruitment. In addition, *in vivo* transactivation assays have demonstrated that 15-keto-PGE_2 preferentially activates PPARγ-LBD-mediated transcription as compared with PPARα and PPARδ. More importantly, the addition of 15-keto-PGE_2 to 3T3-L1 cells can replace the agonist of PPARγ, thereby inducing differentiation of adipocytes efficiently. Altogether, these results show that 15-keto-PGE_2 can function as a PPARγ ligand.

PPARγ was suggested as a nuclear prostanoid receptor

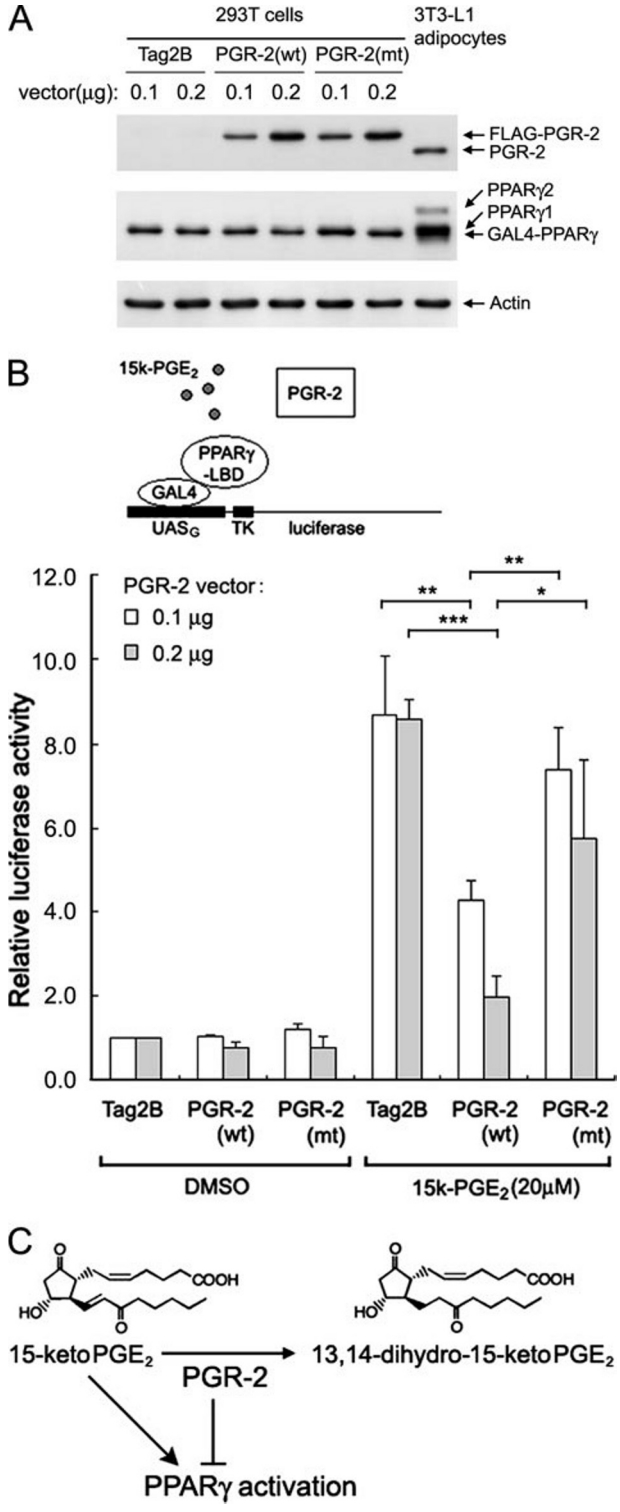

FIGURE 9. **The catalytic function of PGR-2 is required for negative modulation of 15-keto-PGE_2-dependent transcriptional activation of PPARγ.** Wild-type (*wt*) FLAG-PGR-2 but not FLAG-PGR-2/Y259F catalytically defective mutant (*mt*) effectively suppressed PPARγ ligand-binding domain-dependent transactivation. 293T cells were transfected with $UAS_G \times$ 4-TK-LUC (0.7 μg), CMV-βGal (0.1 μg), CMX-GAL4-PPARγ (0.2 μg), and Tag2B, FLAG-PGR-2, or FLAG-PGR-2/Y259F constructs (0.1/0.2 μg) as indicated. Following transfection, cells were treated with dimethyl sulfoxide (*DMSO*; vehicle control), or 20 μM 15-keto-PGE_2 (*15k-PGE*$_2$) for 18 h. After treatment, cells were harvested for Western blot analyses (*A*) and luciferase assays (*B*). For Western blot, equal amounts of cell extracts were analyzed to detect the expression of FLAG-PGR-2 and GAL4-PPARγ in 293T cells and the endogenous levels of PGR-2 and PPARγ in 3T3-L1 adipocytes as indicated. *C*, model for the mechanism by which PGR-2 suppresses 15-keto-PGE_2-dependent transcriptional activation of PPARγ. *, $p < 0.05$; **, $p < 0.01$; ***, $p < 0.001$.

when 15d-PGJ_2, the dehydration product of PGD_2, was first identified as a possible endogenous PPARγ ligand (14, 15). Indeed, 15d-PGJ_2 can drive PPARγ-derived adipocyte differentiation but only at concentrations considerably in excess of those formed endogenously (24, 32). Other compounds formed naturally also possess the capacity to activate PPARγ; among them are 9-HODE, 13-HODE, and 15-hydroxyeicosatetraenoic acid (10, 16), lysophosphatidic acid (17), and nitrolinoleic acid (11). However, it remains to be determined whether the concentrations necessary (IC_{50} values in the *in vitro* ligand binding assay ranging from 1 to 50 μM) are ever attained *in vivo*.

PGE_2 is of particular interest, as it is formed in adipose tissues (33) and is the most abundant prostaglandin formed in preadipocytes. Because a high activity of PGDH has been detected in adipose tissue (21), it seems likely that 15-keto-PGE_2 would be generated in adipocytes.

Here, we have provided diversified lines of evidence consistent with the capacity of 15-keto-PGE_2 to activate PPARγ-dependent adipogenesis. An outstanding question is whether this occurs at concentrations of the metabolite actually formed *in vivo*. At present, it remains a technical challenge to quantify 15-keto-PGE_2 in adipocytes. However, it has been reported that lipid metabolites containing the α,β-unsaturated ketone, including 15-keto-PGE_2, bind to PPARγ covalently, activating PPARγ. Accordingly, it is possible that this covalent binding mechanism enables 15-keto-PGE_2 to activate PPARγ *in vivo* at lower concentrations than would otherwise be the case (34). Further studies will be needed to determine whether PPARγ is actually covalently modified by endogenous concentrations of 15-keto-PGE_2 and whether this modified form accumulates during 3T3-L1 adipocyte differentiation.

This is one of the few examples of a biological functionality attributable to a prostaglandin metabolite rather than to the parent compound. For example, the role of PGDH in closure of the ductus arteriosus (35) is attributable to its capacity to inactivate the parent moiety. The present observations raise the possibility that the increased PGDH but unaltered PPARγ expression in white adipose tissue of *ob*/*ob* mice (36, 37) might reflect a role for 15-keto-PGE_2 in adipogenesis in this model, whereas the recognition that PPARγ can exert its anti-inflammatory effects by ligand-dependent transrepression of inflammatory response genes (38, 39) raises the possibility that macrophage-derived 15-keto-PGE_2 might also modulate adipocyte differentiation and function. Because PGDH is responsible for terminating pro-inflammatory PGE_2 signaling, it will be interesting to know whether the anti-inflammatory capacity of PPARγ in adipose tissue is regulated by catabolic conversion of PGE_2 into 15-keto-PGE_2.

In summary, this study demonstrates for the first time a new link between the catabolism of PGE_2 and the regulation of the PPARγ function. Future studies will determine the importance of this system in the regulation of adipogenesis *in vivo*.

Acknowledgments—We thank Drs. T. K. Tang and S. T. Chen for technical support in the preparation of PGR-2 antibody. We also thank Drs. Kay-Hooi Khoo and Shu-Yu Lin for technical assistance in identifying the in vitro reaction product of PGR-2 by using mass spectrometry at the Core Facilities for Proteomics Research (located at the Institute of Biological Chemistry, Academia Sinica).

REFERENCES

1. Lazar, M. A., and Lehrke, M. (2005) *Cell* **123,** 993–999
2. Evans, R. M., Barish, G. D., and Wang, Y. X. (2004) *Nat. Med.* **10,** 355–361
3. Rosen, E. D., and Spiegelman, B. M. (2001) *J. Biol. Chem.* **276,** 37731–37734
4. Cock, T. A., Houten, S. M., and Auwerx, J. (2004) *EMBO Rep.* **5,** 142–147
5. Westin, S., Kurokawa, R., Nolte, R. T., Wisely, G. B., Mcinerney, E. M., Rose, D. W., Milburn, M. V., Rosenfeld, M. G., and Glass, C. K. (1998) *Nature* **395,** 199–202
6. Desvergne, B., and Wahli, W. (1999) *Endocr. Rev.* **20,** 649–688
7. Nolte, R. T., Wisely, G. B., Westin, S., Cobb, J. E., Lambert, M. H., Kurokawa, R., Rosenfeld, M. G., Willson, T. M., Glass, C. K., and Milburn, M. V. (1998) *Nature* **395,** 137–143
8. Yki-Jarvinen, H. (2004) *N. Engl. J. Med.* **351,** 1106–1118
9. Lehmann, J. M., Moore, L. B., Smith-Oliver, T. A., Wilkison, W. O., Willson, T. M., and Kliewer, S. A. (1995) *J. Biol. Chem.* **270,** 12953–12956
10. Huang, J. T., Welch, J. S., Ricote, M., Binder, C. J., Willson, T. M., Kelly, C., Witztum, J. L., Funk, C. D., Conrad, D., and Glass, C. K. (1999) *Nature* **400,** 378–382
11. Schopfer, F. J., Lin, Y., Baker, P. R., Cui, T., Garcia-Barrio, M., Zhang, J., Chen, K., Chen, Y. E., and Freeman, B. A. (2005) *Proc. Natl. Acad. Sci. U. S. A.* **102,** 2340–2345
12. Shibata, T., Kondo, M., Osawa, T., Shibata, N., Kobayashi, M., and Uchida, K. (2002) *J. Biol. Chem.* **277,** 10459–10466
13. Gilroy, D. W., Colville-Nash, P. R., Willis, D., Chivers, J., Paul-Clark, M. J., and Willoughby, D. A. (1999) *Nat. Med.* **5,** 698–701
14. Forman, B. M., Tontonoz, P., Chen, J., Brun, R. P., Spiegelman, B. M., and Evans, R. M. (1995) *Cell* **83,** 803–812
15. Kliewer, S. A., Lenhard, J. M., Willson, T. M., Patel, I., Morris, D. C., and Lehmann, J. M. (1995) *Cell* **83,** 813–819
16. Nagy, L., Tontonoz, P., Alvarez, J. G., Chen, H., and Evans, R. M. (1998) *Cell* **93,** 229–240
17. McIntyre, T. M., Pontsler, A. V., Silva, A. R., St. Hilaire, A., Xu, Y., Hinshaw, J. C., Zimmerman, G. A., Hama, K., Aoki, J., Arai, H., and Prestwich, G. D. (2003) *Proc. Natl. Acad. Sci. U. S. A.* **100,** 131–136
18. Funk, C. D. (2001) *Science* **294,** 1871–1875
19. Harris, S. G., Padilla, J., Koumas, L., Ray, D., and Phipps, R. P. (2002) *Trends Immunol.* **23,** 144–150
20. Tai, H. H., Ensor, C. M., Tong, M., Zhou, H., and Yan, F. (2002) *Prostaglandins Other Lipid Mediat.* **68–69,** 483–493
21. Anggard, E., Larsson, C., and Samuelsson, B. (1971) *Acta Physiol. Scand.* **81,** 396–404
22. Rosen, O. M., Smith, C. J., Hirsch, A., Lai, E., and Rubin, C. S. (1979) *Recent Prog. Horm. Res.* **35,** 477–499
23. Hyman, B. T., Stoll, L. L., and Spector, A. A. (1982) *Biochim. Biophys. Acta* **713,** 375–385
24. Bell-Parikh, L. C., Ide, T., Lawson, J. A., McNamara, P., Reilly, M., and FitzGerald, G. A. (2003) *J. Clin. Investig.* **112,** 945–955
25. Shivanandappa, T., and Venkatesh, S. (1997) *Anal. Biochem.* **254,** 57–61
26. Yokomizo, T., Ogawa, Y., Uozumi, N., Kume, K., Izumi, T., and Shimizu, T. (1996) *J. Biol. Chem.* **271,** 2844–2850
27. Ensor, C. M., Zhang, H., and Tai, H. H. (1998) *Biochem. J.* **330,** 103–108
28. Hori, T., Yokomizo, T., Ago, H., Sugahara, M., Ueno, G., Yamamoto, M., Kumasaka, T., Shimizu, T., and Miyano, M. (2004) *J. Biol. Chem.* **279,** 22615–22623
29. Richelsen, B. (1991) *Dan. Med. Bull.* **38,** 228–244
30. Glass, C. K., and Rosenfeld, M. G. (2000) *Genes Dev.* **14,** 121–141
31. Hamm, J. K., Park, B. H., and Farmer, S. R. (2001) *J. Biol. Chem.* **276,** 18464–18471
32. Tzameli, I., Fang, H., Ollero, M., Shi, H., Hamm, J. K., Kievit, P., Hollenberg, A. N., and Flier, J. S. (2004) *J. Biol. Chem.* **279,** 36093–36102
33. Fain, J. N., Madan, A. K., Hiler, M. L., Cheema, P., and Bahouth, S. W. (2004) *Endocrinology* **145,** 2273–2282
34. Shiraki, T., Kamiya, N., Shiki, S., Kodama, T. S., Kakizuka, A., and Jingami, H. (2005) *J. Biol. Chem.* **280,** 14145–14153
35. Coggins, K. G., Latour, A., Nguyen, M. S., Audoly, L., Coffman, T. M., and Koller, B. H. (2002) *Nat. Med.* **8,** 91–92
36. Soukas, A., Cohen, P., Socci, N. D., and Friedman, J. M. (2000) *Genes Dev.* **14,** 963–980
37. Vidal-Puig, A., Jimenez-Liñan, M., Lowell, B. B., Hamann, A., Hu, E., Spiegelman, B., Flier, J. S., and Moller, D. E. (1996) *J. Clin. Investig.* **97,** 2553–2561
38. Xu, H., Barnes, G. T., Yang, Q., Tan, G., Yang, D., Chou, C. J., Sole, J., Nichols, A., Ross, J. S., Tartaglia, L. A., and Chen, H. (2003) *J. Clin. Investig.* **112,** 1821–1830
39. Pascual, G., Fong, A. L., Ogawa, S., Gamliel, A., Li, A. C., Perissi, V., Rose, D. W., Willson, T. M., Rosenfeld, M. G., and Glass, C. K. (2005) *Nature* **437,** 759–763